Hindawi
Shock and Vibration
Volume 2021, Article ID 6688964, 15 pages
https://doi.org/10.1155/2021/6688964

Research Article

Analysis on the Difference of Impact Response between Single Coal-Rock Particle and the Box Structure-Based Tail Beam

Li-rong Wan, Zhe Li, Yang Yang, and Ran Li

College of Mechanical and Electronic Engineering, Shandong University of Science and Technology, Qingdao 266590, China

Correspondence should be addressed to Yang Yang; sdkdyangyang@126.com

Received 16 October 2020; Accepted 5 January 2021; Published 4 February 2021

Academic Editor: Lei Su

In the process of coal caving, the basis of identifying coal and rock by the vibration signal is the difference of the tail beam response when coal-rock impacts the tail beam, and the tail beam in the hydraulic support is a complex box structure with multiplate transverse and longitudinal welding, and the response difference of the box structure-based tail beam under the impact of coal-rock is not clear. Therefore, this paper studies the response difference of box structure-based tail beam when coal-rock particle impacts on the box structure-based tail beam. Firstly, through the construction and analysis of the impact theoretical model of the coal-rock particle and metal plate, it is found that the complex box structure of the tail beam makes it extremely difficult to establish the impact theoretical model of the coal-rock and box structure-based tail beam, so it is impossible to directly study the response of the box structure-based tail beam when the coal-rock impacts on the box structure-based tail beam by the theoretical method. Therefore, the impact simulation model of coal-rock particle and box structure-based tail beam is further established. Through the changes of kinetic energy and internal energy of the box structure-based tail beam system, the contact response of collision contact zone, and noncollision contact zone of the box structure-based tail beam, the response difference of box structure-based tail beam when coal-rock particle impacts on the box structure-based tail beam is analyzed. Then, by changing the impact speed and contact mode of the coal-rock particle, the effects of impact speed and the contact mode on the response difference of the box structure-based tail beam are studied separately. The conclusion shows that the response difference of the box structure-based tail beam under the impact of the coal particle and rock particle is obvious, and the difference increases as the impact speed increases, and the difference increases as the contact range increases.

1. Introduction

As an important reserve resource in the world, coal is one of the irreplaceable energy sources in human production and life. For example, coal consumption accounts for as much as 59% of China's annual energy consumption structure [1]. In general, thick coal seam accounts for a large proportion of coal reserves, so fully mechanized mining top-coal caving technology [2–6] has been widely used in coal mining, and fully mechanized mining equipment has gradually improved its overall performance in application. However, in the process of top-coal caving, manual judgment is still used to control the opening switch of drawing coal, which affects the coal caving efficiency and personnel safety to a certain extent, so it is necessary to improve the intelligent and unmanned coal-caving process [7].

In the process of exploring the intelligent and unmanned process of coal caving, coal-rock identification technology has received widespread attention as a crucial step. Wang et al. proposed a new method of coal-gangue separation based on laser triangulation and weight, using three-dimensional laser scanning technology to calculate the density from the volume [8]. By establishing the difference of coal-gangue surface texture and gray level, Hou proposed a method that combines image features with the artificial neural network to identify coal gangue [9]. Sun et al. proposed a coal-rock interface detection method by using digital image analysis technology based on the difference of coal and rock texture characteristics [10, 11]. He et al. measured the spectral reflectance of coal and rock and applied multispectral remote-sensing images to detect coal mine areas [12]. Mao et al. proposed a rapid coal classification method

based on infrared spectroscopy by measuring spectral data of coal gangue with spectrometer [13, 14]. Dou et al. used the SVM coal-gangue recognition method based on image analysis; the SVM method is used to identify and select the optimal image features, so as to reduce the optimal features and improve the class accuracy [15]. Zhang et al. carried out an exploratory study using machine vision to simultaneously detect multiple information of coal quality online, including particle size distribution, density distribution, the ash content of each density fraction, and total ash content [16]. Taking the sound signal and vibration signal as the analysis object, Si et al. combined the improved radical basis function neural network with Dempster–Shafer evidence theory and proposed a fusion recognition method for the coal and rock cutting state of the shearer [17, 18]. The above is an exploration of coal-rock recognition based on images, rays, and acoustic signals, but many external factors such as noisy environment and dark light in the process of coal caving will make the recognition effect worse.

In order to overcome the influence of the external environment, many scholars have explored coal-rock recognition based on vibration signals. Liu et al. proposed a vibration feature extraction method based on the Hilbert spectrum information center and applied Mahalanobis distance measurement to the Hilbert spectrum information entropy of the vibration signal to effectively detect the coal-rock interface [19, 20]. Taking the vibration signal of the tail beam of the hydraulic support as the research point, Li et al. constructed the feature vector with the fractal box dimension and wavelet packet energy moment as the input vector of the BP neural network to identify coal and rock [21]. Wang and Zhang proposed a new method for dynamic recognition of coal-rock interface based on adaptive weight optimization and multi-information fusion of current, temperature, sound, and vibration signals [22]. Yang et al. used the time-domain characteristic calculation and HHT processing of the vibration acceleration signal of coal gangue impacting the metal plate, and the coal-gangue recognition accuracy rate obtained by the machine learning integration algorithm was high [23, 24]. Coal-gangue identification based on the vibration signal is more suitable for coal-gangue identification in the process of coal caving because of its advantages of small environmental interference, easy data acquisition, and high recognition rate [25]. However, most scholars only filter and analyze the vibration signal of the coal-rock impacting the tail beam or analyze the impact of coal-rock particles on the metal plate or the whole hydraulic support. However, they have not analyzed the impact response characteristics of the box structure-based tail beam and lack the basic research on the relevant response characteristics of box structure-based tail beam under coal-rock particle impact.

Based on previous research studies on elastic collision [26–30], this paper takes the box structure-based tail beam as the research object and first establishes the theoretical model of spherical particles impacting the metal plate. Because the response of the box structure-based tail beam is different from that of a single metal plate and is difficult to establish a theoretical model, the simulation model of coal-rock particle impacting the box structure-based tail beam is further established to study the difference of impact response of the box structure-based tail beam when the coal particle and rock particle impact the box structure-based tail beam and the change of impact response difference under the influence of impact speed and contact mode.

2. Theoretical Model of Impact and Collision of the Coal-Rock Particle

In the process of fully mechanized top-coal caving mining, the shape of coal and rock particles is irregular. If a certain irregular shape is used for subsequent research, not only the modeling parameters are too many and the research process is cumbersome but also the results obtained are not representative. The spherical particles can be determined only by radius parameters, and the area of the collision contact zone can be changed by changing radius parameters. Therefore, in the collision contact theoretical model in this paper, the coal and rock particles are equivalent to spherical particles, and the part of the tail beam in contact with the coal and rock is regarded as the metal plate.

Assuming that coal-rock particles are isotropic, completely elastic, have uniform mass and there is no friction on the contact surface between the particles and tail beam, the theoretical model of spherical coal-rock particles impacting the metal plate is established based on Hertz contact.

Contact force:

$$F = \frac{4}{3} \cdot R^{(1/2)} \cdot E \cdot \delta^{(3/2)}. \tag{1}$$

Equivalent modulus:

$$E = \frac{E_1 \cdot E_2}{\left(1 - \mu_1^2\right) \cdot E_2 + \left(1 - \mu_2^2\right) \cdot E_1}. \tag{2}$$

Equivalent radius:

$$R = \frac{R_1 \cdot R_2}{R_1 + R_2}, \tag{3}$$

where δ is the total contact deformation between the metal plate and spherical particles, μ_1 is Poisson's ratio of the metal plate, μ_2 is Poisson's ratio of spherical coal or rock particles, E_1 is the elastic modulus of the metal plate, E_2 is the elastic modulus of spherical coal or rock particles, R_1 is the radius of the metal plate, and R_2 is the radius of spherical coal or rock particles. Since the radius of a plane object is infinite, that is, $R_1 = \infty$, the equivalent radius $R = R_2$.

In practice, there must be friction between the metal plate and coal particles. For the theoretical model to be closer to reality, friction needs to be considered on the basis of the Hertz contact theory. Flores has established a nonlinear spring-damping contact theory considering both elastic force and damping dissipation force of the system [28, 29].

Contact force:

$$F_N = K\delta^n + \chi\delta^n\dot{\delta}. \tag{4}$$

Hysteresis damping factor:

$$\chi = \frac{3K\left(1 - c_r\right)}{2\dot{\delta}^{(-)}}, \tag{5}$$

where K is the generalized stiffness parameter, c_r is the coefficient of restitution, and $\dot{\delta}^{(-)}$ is the initial contact velocity.

Assuming that the metal plate is an independent individual and considering the deformation of the metal plate impacted by particles (as shown in Figure 1), the deflection equation y_{dur} and energy equation W of the metal plate under Hertz contact force are obtained as follows [30]:

$$\begin{aligned} y_{\text{dur}} &= \frac{F_N x_1 x_2}{6E_2 I_2 L} \cdot \left(L^2 - x_1^2 - x_2^2\right), \\ W &= \frac{F_N^2 x_1 x_2}{12E_2 I_2 L} \cdot \left(L^2 - x_1^2 - x_2^2\right), \end{aligned} \tag{6}$$

where I_2 is the moment of inertia of the metal plate, L is the length of the metal plate, and x_1 and x_2 are the distances from the left end of the metal plate and the right end of the metal plate to the impact point.

Based on the above theory, Yang et al. studied the contact response of the system when multiple coal and rock particles impacted the metal plate [30], which indirectly demonstrated the availability of the contact theoretical model. The above theory is suitable for particles impacting a single metal plate, but the theoretical research of the overall structure of the box structure-based tail beam is not completely the same as the theoretical study of the single metal plate mentioned above. The complexity is that multiple metal plates are welded horizontally and longitudinally to form multiple box spaces in the tail beam structure (as shown in the cross-sectional view of the box structure-based tail beam in Figure 2, only part of the metal plates are marked). When plate 1 is impacted by coal and rock particles, metal plates such as plates 2–4 directly connected with plate 1 will affect it, and plate 5 will also affect plate 2 and plate 3 and thus indirectly affecting plate 1. It is extremely difficult to establish a theoretical model of the box structure-based tail beam impacted by coal and rock particles if the degree of mutual influence between the extension degrees of freedom, bending deflection, rotation degrees of freedom, and section deformation degrees of freedom between the various metal plates and their influence factors are considered at the same time [31, 32].

3. Simulation Model of Impact between the Coal-Rock Particle and Box Structure-Based Tail Beam

Since it is extremely difficult to establish a theoretical model of particle impact on the box structure-based tail beam, the impact simulation model of coal-rock particles and the box structure-based tail beam is established to further study the collision response of the box structure-based tail beam under the impact of coal-rock particles. The top-coal caving hydraulic support (as shown in Figure 3) mainly includes top beam, shield beam, linkage, base, and tail beam, which are

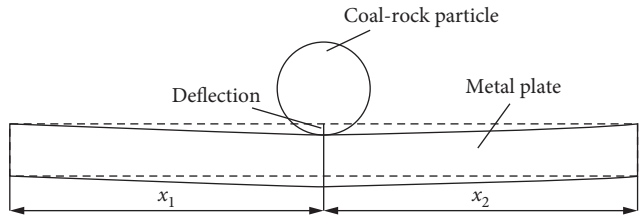

Figure 1: The deformation diagram of the metal plate under impact.

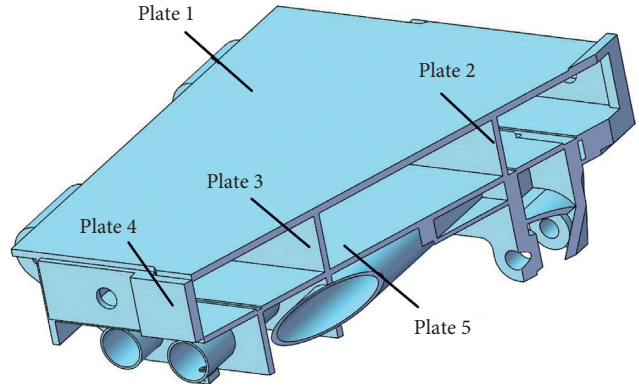

Figure 2: The sectional view of the box structure-based tail beam.

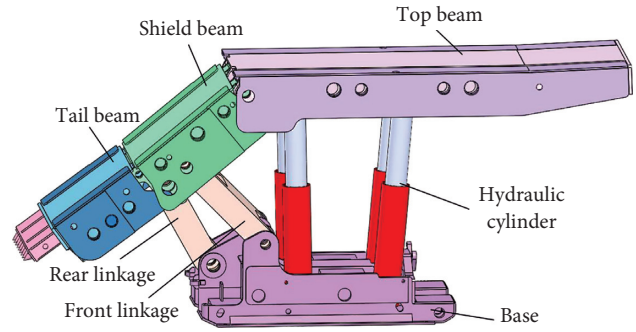

Figure 3: The model of the top-coal caving hydraulic support.

essential equipment in fully mechanized coal caving technology. The biggest difference between the top-coal caving hydraulic support and ordinary hydraulic support is that the coal drawing mechanism is added. The coal drawing mechanism (as shown in Figure 4) is mainly composed of tail beam, insert plate, tail beam jack, insert plate jack, side plates, and other components. Among them, the tail beam and plug-in plate are the main parts to realize coal caving, gangue blocking, and coal crushing, and the side plates can prevent coal and rock from falling into the hydraulic support to a certain extent. Considering that the tail beam, insert plate, and side plates are all subjected to the impact of coal-rock particles, the position and quality of the insert plate and side plates may affect the simulation results. Therefore, the tail beam, insert plate, and side plates of the hydraulic support are taken as a whole to construct the simulation model.

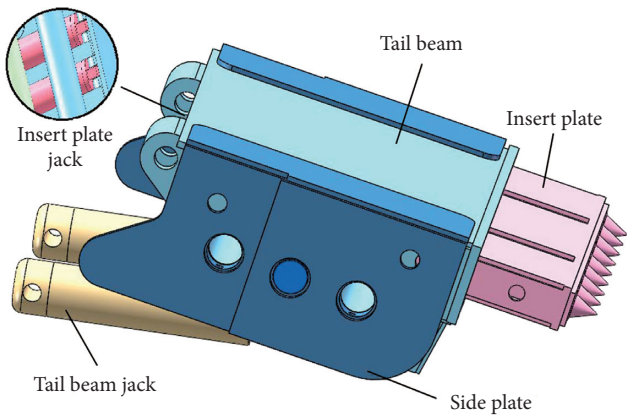

Figure 4: The coal-drawing mechanism.

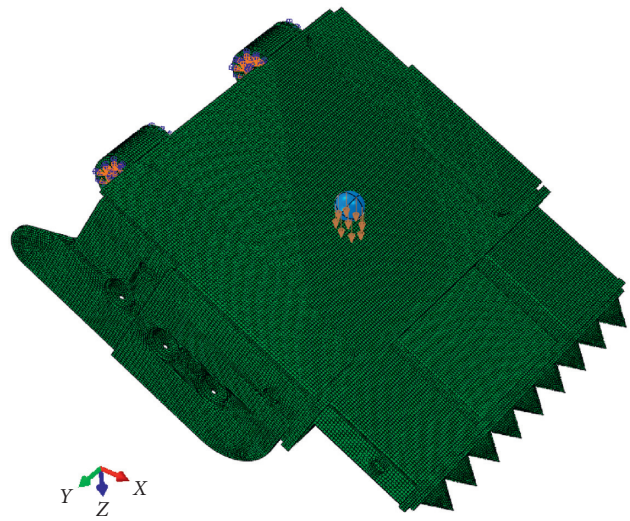

Figure 5: The simulation model of the coal-rock particle impacting the box structure-based tail beam.

Since this paper is not the study of the entire coal caving mechanism, but a box structure-based tail beam as the main research object, it does not consider the force exerted by the tail beam jack on the box structure-based tail beam and only considers the impact response of coal-rock impact to the box structure-based tail beam in a fixed state. Therefore, when the simulation model was established, only fixed constraints were set at the hinge point of the tail beam and shield beam to ensure that the box structure-based tail beam was fixed in space. To make the simulation results more accurate, the tail beam is divided into a hexahedral mesh with better quality, the element type is C3D8R, and the simulation type displays dynamic simulation. Gravity acceleration of 9.8 m/s^2 is applied to both the coal-rock particle and box structure-based tail beam, and the impact speed direction of the coal-rock particle is in the positive direction of the Z-axis of the system coordinate axis (vertically downward), and the simulation time is 0.005 s. The simulation model diagram is shown in Figure 5.

4. Difference Analysis of the Coal-Rock Particle Impacting the Box Structure-Based Tail Beam

4.1. Response Difference of the Box Structure-Based Tail Beam Impacted by Coal and Rock

4.1.1. Analysis of Impact Response of the Box Structure-Based Tail Beam in the Collision Contact Zone. In the process of coal caving, the basis for judging whether to stop coal caving is the mixture ratio of coal and rock. When the rock content is relatively large, the tail beam will be raised to prevent the rock at the top from sliding continuously. The coal-rock identification system based on the vibration signal can distinguish the mixing of coal and rock through the different responses of the tail beam when coal-rock impacts. Therefore, it is necessary to study the difference of the impact response of the tail beam when the coal particles and rock particles impact the tail beam. Based on the aforementioned simulation model, create spherical coal particles and rock particles with the same volume ($R = 0.05$ m) and set the impact velocity to 5 m/s and the simulation time to 0.005 s. The system kinetic energy and internal energy are obtained, as shown in Figure 6.

From Figure 6, under the impact of the rock particle, the system has more residual kinetic energy and the variation range of residual kinetic energy is about 12 J, and the peak value of the system internal energy curve is large and the internal energy of the stable state is about 4 J; under the impact of the coal particle, the system residual kinetic energy is less and the variation range of residual kinetic energy is about 7.5 J, and the peak value of the system internal energy curve is small and the internal energy of the stable state is about 2 J. At the same time, the system kinetic energy and system internal energy of the rock particle impacting the box structure-based tail beam are always greater than that of the coal particle impacting the box structure-based tail beam. In the initial stage of impact collision, the downward slope of the system kinetic energy curve of the rock particle impacting the box structure-based tail beam is greater than that of the coal particle, but the arrival time of the valley value (the lowest point value of the curve) is consistent; the slope of the system internal energy curve of the rock particle impacting the box structure-based tail beam is greater than that of the coal particle, but the peak arrival time is consistent. In the later stage of impact collision, the system kinetic energy curve of the rock particle impacting the box structure-based tail beam oscillates more obviously, and the system kinetic energy curve of the coal particle impacting the box structure-based tail beam oscillates more smoothly; the oscillation amplitude of the system internal energy curve of the rock particle impacting the box structure-based tail beam is larger than that of the coal particle.

According to the above analysis of system kinetic energy and internal energy, the system kinetic energy and internal energy have obvious different response changes when the coal-rock particles impact the box structure-based tail beam. In order to further study the difference of the impact response of the box structure-based tail beam when coal-rock particles impact the box structure-based

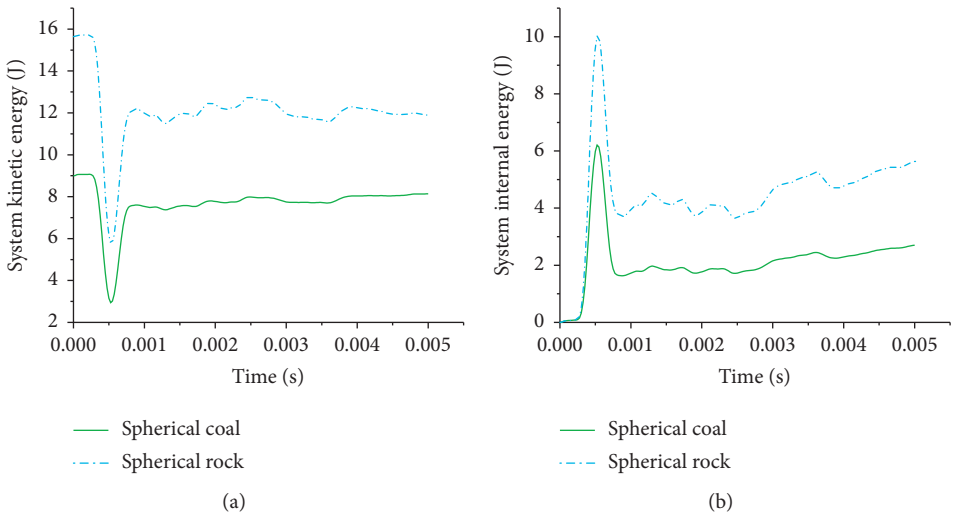

Figure 6: (a) System kinetic energy and (b) system internal energy under the impact of coal-rock particles.

tail beam, this paper analyzes the dynamic response analysis in the collision contact zone of the coal-rock particles impacting the box structure-based tail beam, and 25 nodes are selected in the collision contact zone, the Z-direction velocities of the 25 nodes are extracted, and the average value is calculated. The curve of the average velocity change of the nodes in the tail beam collision contact zone is drawn, as shown in Figure 7.

It can be seen from Figure 7 that the peak value of the average velocity curve of the tail beam collision contact zone under the impact of the rock particle is greater than that under the impact of the coal particle, but the peak arrival time of both is the same. In the later stage of the collision, the oscillation amplitude of the average velocity curve of the rock particle impacting the box structure-based tail beam is obviously greater than that of the coal particle impacting the box structure-based tail beam. This is because the density of rock is greater than that of coal, the mass of rock particles is larger in the same volume, the impact kinetic energy is greater when the impact velocity is the same, and the box structure-based tail beam absorbs more energy during the collision process, so the vibration response of the box structure-based tail beam under the impact of the rock particle is obviously stronger than that under the impact of the coal particle.

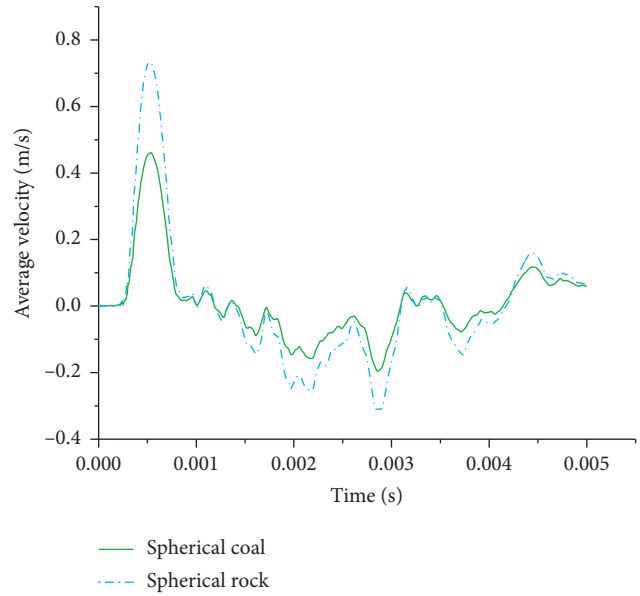

Figure 7: Average velocity in the tail beam collision contact zone under the coal-rock particle impact.

4.1.2. Analysis of Impact Response in the Noncollision Contact Zone of the Box Structure-Based Tail Beam. In the actual signal collection process of coal-rock particles impacting the box structure-based tail beam, the signal collection position is fixed, while the coal-rock impact position is variable, so the information collection position will be in the tail beam noncollision contact zone, and the vibration response of the collision contact zone is different from that of the noncollision contact zone. Therefore, in order to further analyze the dynamic response difference of the box structure-based tail beam under the impact of coal-rock particles, four nodes in the noncollision contact zone are selected for analysis, and the node positions are shown in Figure 8. The obtained nodal acceleration curve is shown in Figure 9, the nodal velocity curve is shown in Figure 10, and the nodal displacement curve is shown in Figure 11.

According to Figures 9–11, under the impact of the coal particle, the nodal acceleration vibration frequency of the noncollision contact zone of the box structure-based tail beam is low, and the vibration amplitude is small; under the impact of the rock particle, the acceleration vibration frequency is high, and the vibration amplitude is the largest; the vibration amplitude of the nodal acceleration curve at the lower side of the box structure-based tail beam is larger than that of the upper side. The nodal velocity curve under the rock particle impacts has a larger peak value and amplitude, while the nodal velocity curve under the coal particle

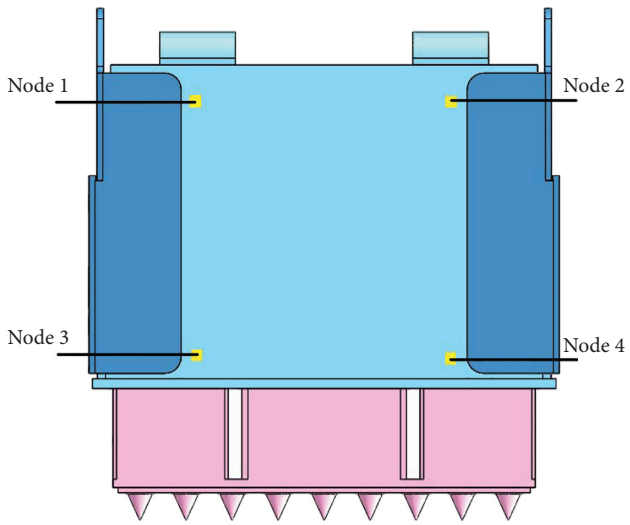

Figure 8: Nodal position in the tail beam noncollision contact zone.

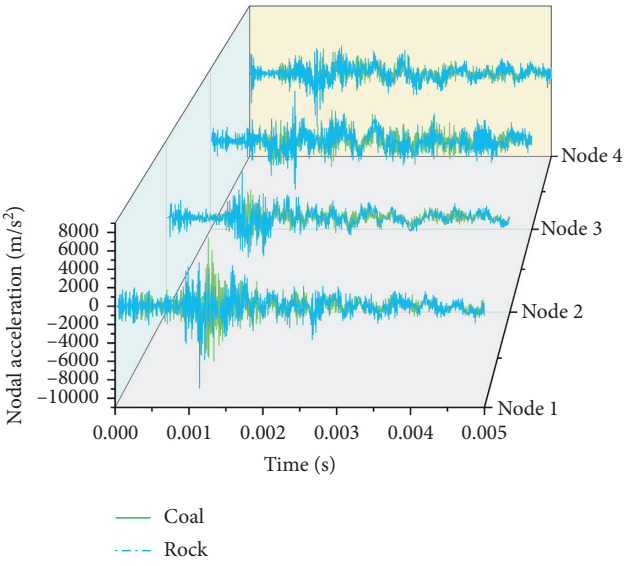

Figure 9: Nodal acceleration in the tail beam noncollision contact zone under the impact of coal-rock particles.

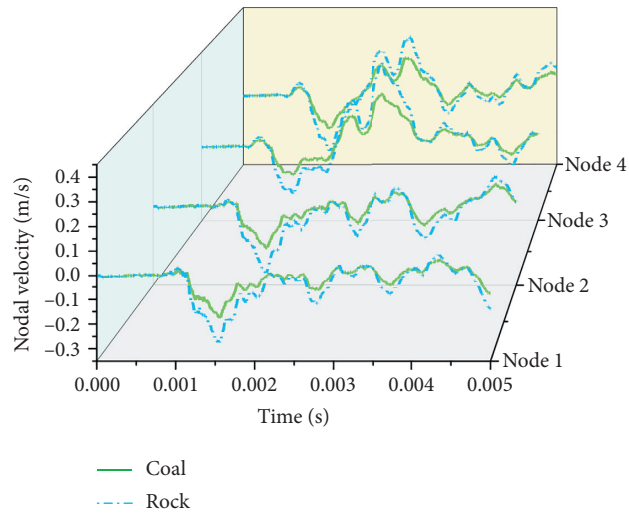

Figure 10: Nodal velocity in the tail beam noncollision contact zone under the impact of coal-rock particles.

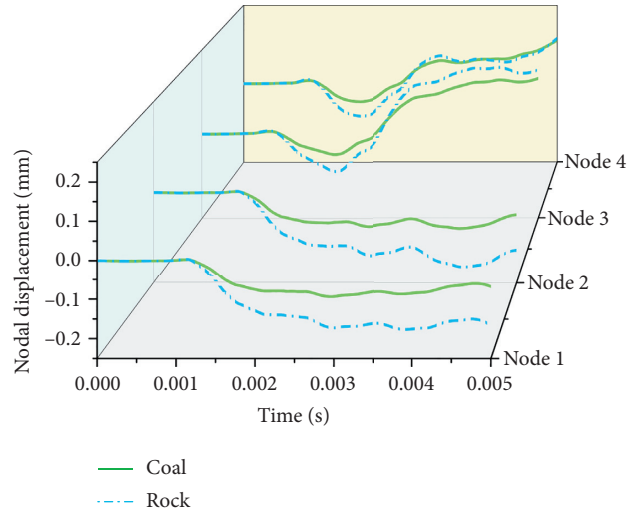

Figure 11: Nodal displacement in the tail beam noncollision contact zone under the impact of coal-rock particles.

impacts has a smaller peak value and small amplitude; the velocity of the nodes on the upper side of the box structure-based tail beam is lower, and the negative value accounts for more, while the velocity of the nodes on the lower side of the box structure-based tail beam is higher, and the positive value accounts for more. When coal-rock particles impact the box structure-based tail beam, the upper nodes of the box structure-based tail beam first move in the negative direction of z-axis and then move in the positive direction of z-axis, and the lower nodes always move in the negative direction of z-axis; the displacement of upper nodes of the box structure-based tail beam under the impact of the rock particle is larger and faster than that under the impact of the coal particle, and the displacement of the lower nodes of the box structure-based tail beam changes faster under the impact of the rock particle than that under the impact of the coal particle, but it is similar in the later stage of collision. The results show that the response of the tail beam noncollision contact zone is obviously different when the coal and rock particle impact the box structure-based tail beam.

4.2. Influence of Impact Speed on the Impact Response Difference of the Box Structure-Based Tail Beam Impacted by Coal-Rock

4.2.1. Analysis of Impact Response in the Collision Contact Zone. In the process of top-coal caving, the falling height of coal-rock particles is different, which results in different speeds of coal-rock particles impacting the tail beam. Therefore, the impact speed of the coal-rock particles is changed in the simulation model to study the influence of

impact speed of the coal-rock particles on the impact response of the box structure-based tail beam. Take the speed of the coal-rock particles as 2 m/s, 3 m/s, 4 m/s, and 5 m/s and get the system kinetic energy and system internal energy, as shown in Figure 12.

According to Figure 12, with the decrease of impact speed, the system kinetic energy and internal energy decrease as a whole, the valley value of the system kinetic energy curve and the peak value of the system internal energy curve decrease, and the arrival time of both of them is delayed, and the oscillation in the back section of the curve is weakened. With the increase of impact speed, the energy gap between the coal-rock particles continues to increase, and the vibration of the energy curve under the impact of the rock particle is more obvious and greater than that under the impact of the coal particle. In order to further analyze the dynamic characteristics of the box structure-based tail beam, the 25 nodes in the tail beam collision contact zone are taken as the research objects, and the Z-direction velocities at 4 different impact speeds are extracted, and the average velocity curve is drawn, as shown in Figure 13.

According to Figure 13, when the coal-rock particles with different speeds impact the box structure-based tail beam, the change in the average velocity of the tail beam collision contact zone is as follows: with the increase of impact speed, the velocity peak value increases, peak arrival time advances, velocity slope increases at the initial stage of collision, and curve amplitude increases at the later stage of collision. With the continuous increase of the impact speed, the peak gap of the average velocity of the tail beam collision contact zone under the impact of the rock particle and coal particle continues to increase, and the gap of the velocity oscillations' amplitude in the later stage of collision increases. Based on the above results, the difference in impact response of the collision contact zone of the box structure-based tail beam under the impact of the rock particle and coal particle is more obvious with the increase of impact speed.

4.2.2. Analysis of Impact Response in the Noncollision Contact Zone. In order to further explore the response difference of impact speed to coal-rock particles impacting the box structure-based tail beam, four nodes in the tail beam noncollision contact zone in the previous section are selected as the research objects. The nodal acceleration at the speeds of 2 m/s, 3 m/s, 4 m/s, and 5 m/s are extracted, respectively, and the curve is shown in Figure 14, nodal velocity curve is shown in Figure 15, and nodal displacement curve is shown in Figure 16.

It can be seen from Figures 14–16 that, under the impact of the coal-rock particles with impact speeds of 2 m/s, 3 m/s, and 4 m/s, the law of acceleration, velocity, and displacement in the noncollision contact zone is similar to that when the impact speed is 5 m/s. With the increase of impact speed, the acceleration vibration amplitude in the noncollision contact zone of the box structure-based tail beam under the impact of the coal particle and rock particle increases, and the difference between them increases; the difference between the peak of the average velocity curve in the tail beam noncollision contact zone under the impact of the coal particle and rock particle becomes larger, the peak arrival time is gradually advanced, and the curve amplitude is more obvious, and the difference between the maximum velocity of the nodes on the upper side of the box structure-based tail beam and that on the lower side becomes larger; the difference of the displacement curve in the noncollision contact zone under the impact of the coal particle and rock particle becomes larger, and the displacement difference of the nodes on the upper side of the box structure-based tail beam is more obvious than that on the lower side. Based on the above phenomenon, it can be seen that the impact speed does not change the overall law of the impact response in the noncollision contact zone of the box structure-based tail beam, but the increase of impact speed makes the impact response difference of the noncollision contact zone more obvious under the impact of the rock particle and coal particle.

4.3. Influence of the Contact Mode on the Impact Response Difference of the Box Structure-Based Tail Beam Impacted by Coal-Rock

4.3.1. Analysis of Impact Response in the Collision Contact Zone. Due to the irregularity of coal-rock particles, when they collide with the box structure-based tail beam, there are three typical collision contact modes: point contact, line contact, and surface contact. In order to study the influence of the contact mode on the impact response difference of coal-rock impacting the box structure-based tail beam, three kinds of particles with the same volume and different shapes, namely, spherical particles, cylindrical particles, and square particles, were established to simulate the point contact, line contact, and surface contact in the process of impact, respectively. The particle parameters are shown in Table 1. Set the particle impact speed to 5 m/s, and obtain the system kinetic energy and internal energy, as shown in Figure 17.

According to Figure 17, at the initial stage of particle impact, when the point contacts, the slope of the system kinetic energy curve is the smallest, valley value of the curve is the smallest, and arrival time of the valley value is the latest, and the slope of the system kinetic energy curve is the smallest, peak value is the largest, and arrival time of the peak is the latest; when the line contacts, the slope of the system kinetic energy curve is small, valley value of the curve is small, and arrival time of the valley value is moderate, and the slope of the system kinetic energy curve is small, peak value is small, and arrival time of the peak is moderate; when the surface contacts, the slope of the system kinetic energy curve is the largest, valley value of the curve is the largest, and arrival time of the valley value is the earliest, and the

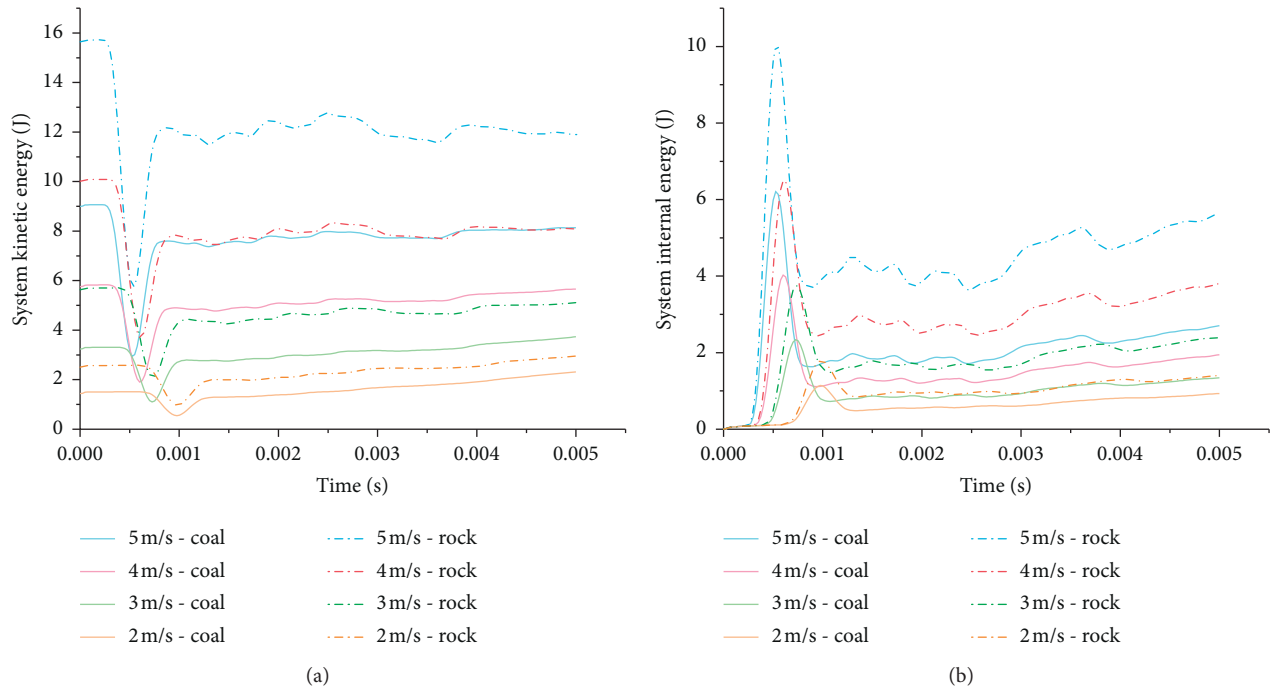

Figure 12: (a) System kinetic energy and (b) system internal energy under different impact speeds.

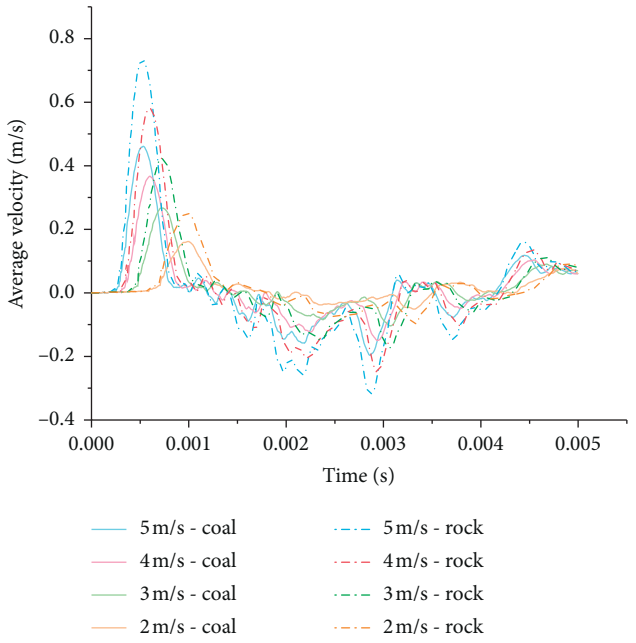

Figure 13: Average velocity in the tail beam collision contact zone under different impact speeds.

slope of the system kinetic energy curve is the largest, peak value is the smallest, and arrival time of the peak is the earliest. At the later stage of coal-rock particle impact, the system kinetic energy is the largest and the system internal energy is the smallest during the point contact, the system kinetic energy is the smallest and the system internal energy is the largest during the surface contact, and the system kinetic energy and internal energy are in the middle during the line contact. When the contact mode is the same, the system kinetic energy and system internal energy under the impact of the rock particle are always greater than those under the impact of the coal particle.

Taking the 25 nodes in the collision contact zone of the aforementioned as the research object, extract the Z-direction velocity and draw the average velocity curve, as shown in Figure 18. It can be seen from Figure 18 that when coal-rock particles impact the box structure-based tail beam with different contact modes, the average velocity changes in the tail beam contact zone are shown as follows: the peak value of the average velocity curve is the smallest, and the arrival time is the slowest during the point contact; the peak value of the average velocity curve is small, and the arrival time is slow during the line contact; the peak value of the average velocity curve is the largest, and the arrival time is the fastest during the surface contact. When the contact mode is the same, the vibration of the velocity curve in the tail beam contact zone under the impact of the rock particle is more severe than that under the impact of the coal particle, and the vibration gap is the largest in the surface contact, the second in the line contact, and the least in the point contact.

4.3.2. Analysis of Impact Response in the Noncollision Contact Zone. In order to further analyze the response difference of the contact mode to the impact of coal-rock particles on the box structure-based tail beam, four nodes in the tail beam noncollision contact zone are taken as the research object, and the nodal acceleration under the three contact modes are extracted, respectively, and the curves are drawn, as shown in Figure 19, and the curve of node velocity

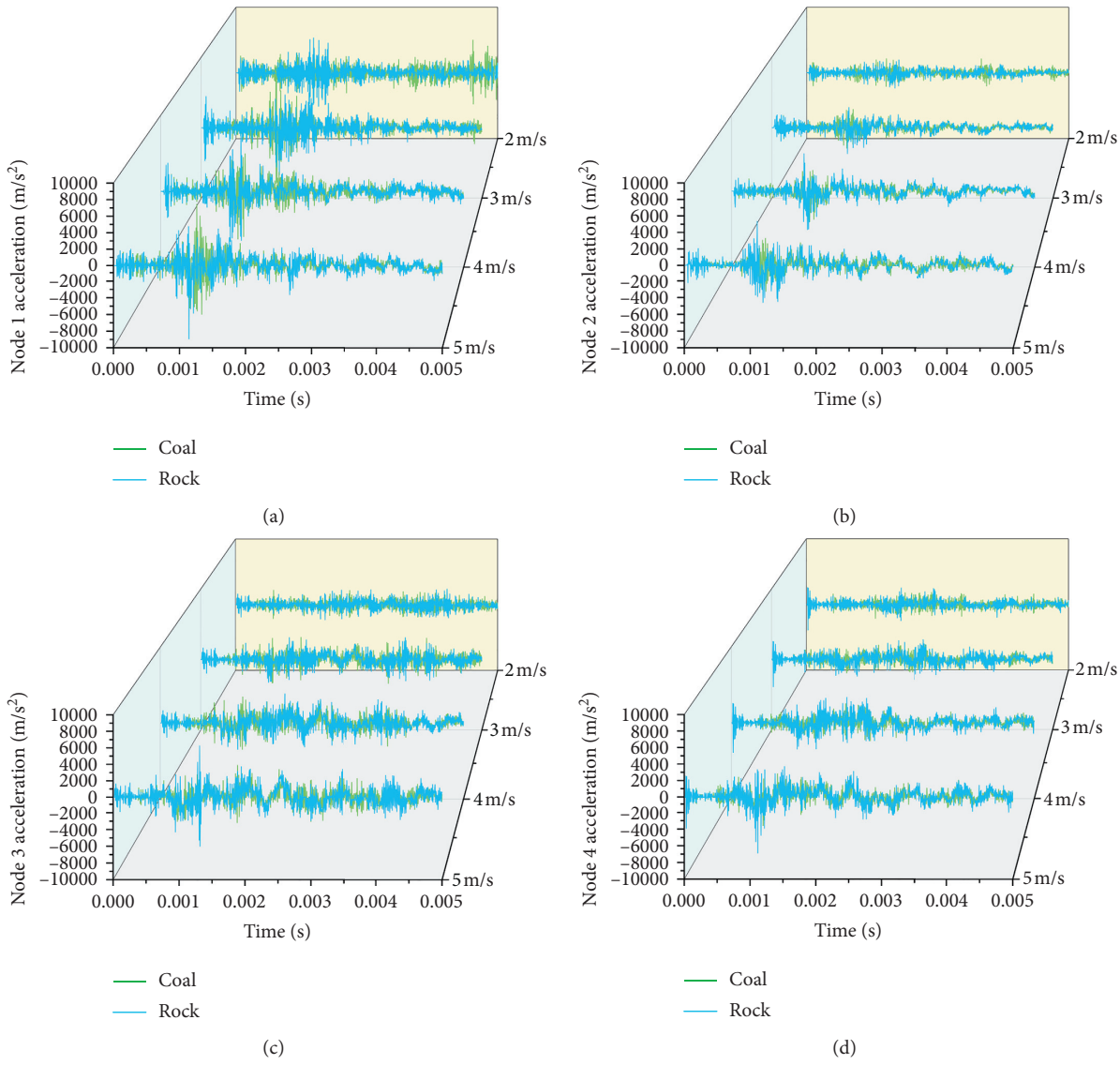

Figure 14: Nodal acceleration in the tail beam noncollision contact zone under different impact speeds: (a) Node 1 acceleration; (b) Node 2 acceleration; (c) Node 3 acceleration; (d) Node 4 acceleration.

is shown in Figure 20, and the curve of node displacement is shown in Figure 21.

It can be seen from Figure 19 that when coal-rock particles impact the box structure-based tail beam in different contact modes, the nodal accelerations in the tail beam noncollision contact zone are all shown as follows: the vibration frequency and amplitude of nodal acceleration are the lowest during the point contact, vibration frequency and amplitude of nodal acceleration are moderate during the line contact, acceleration vibration frequency is the highest, and vibration amplitude is the largest during the surface contact. When the coal-rock particles impact the box structure-based tail beam in the same contact mode, the nodal acceleration amplitude of the tail beam noncollision contact zone under the impact of the rock particle is larger and more frequent than that under the impact of the coal particle. And, the vibration gap is the most obvious in the surface contact, the second in the line contact, and the least in the point contact.

It can be seen from Figure 20 that when the coal-rock particles impact the box structure-based tail beam with different contact modes, the nodal velocity in the tail beam noncollision contact zone is shown as follows: in the case of point contact, the nodal velocity response is the slowest and the peak value is the smallest; in the case of surface contact, the nodal velocity response is the fastest and the peak value is the highest; in the case of line contact, the response speed

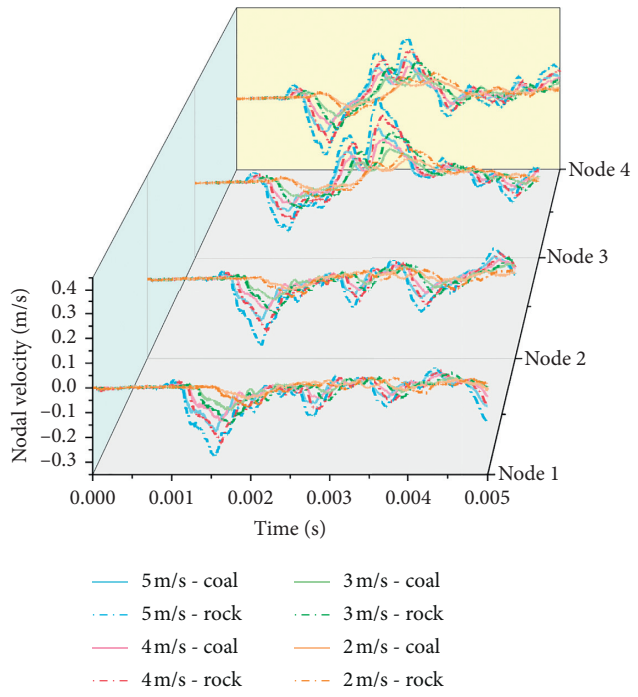

Figure 15: Nodal velocity in the tail beam noncollision contact zone under different impact speeds.

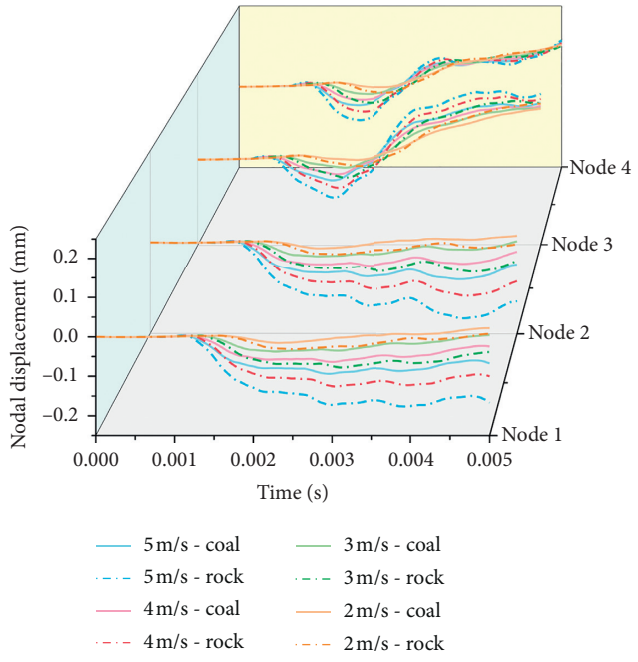

Figure 16: Nodal displacement in the tail beam noncollision contact zone under different impact speeds.

Table 1: Impact parameters of the coal-rock particle.

Particle	Spherical particle	Cylindrical particle	Square particle
Size (m)	$R = 0.05$	$R = 0.0408$; $L = 0.1$	$L = 0.0806$

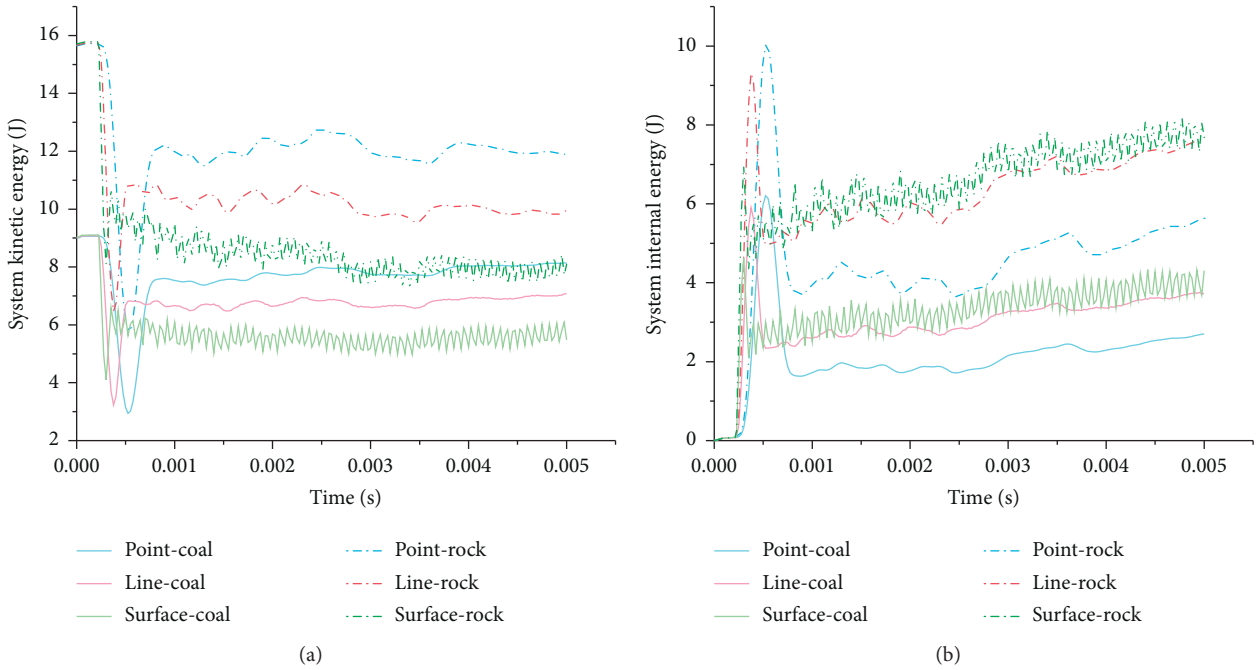

Figure 17: (a) System kinetic energy and (b) system internal energy under different contact modes.

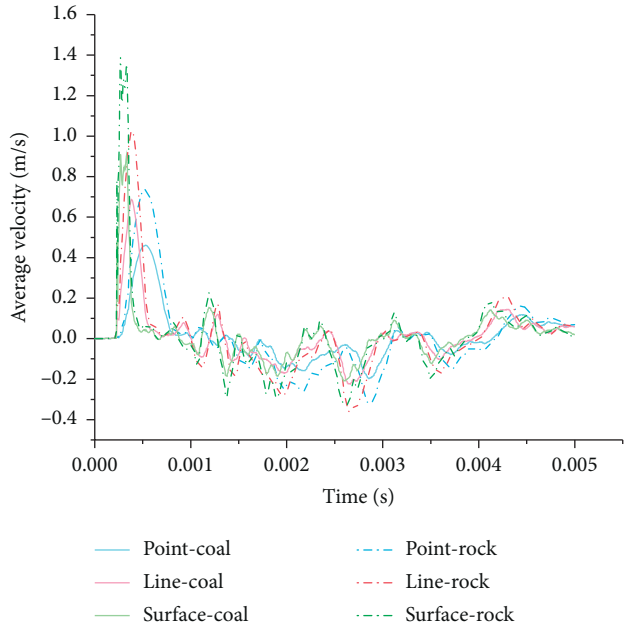

Figure 18: Average velocity of nodes in the tail beam collision contact zone under different contact modes.

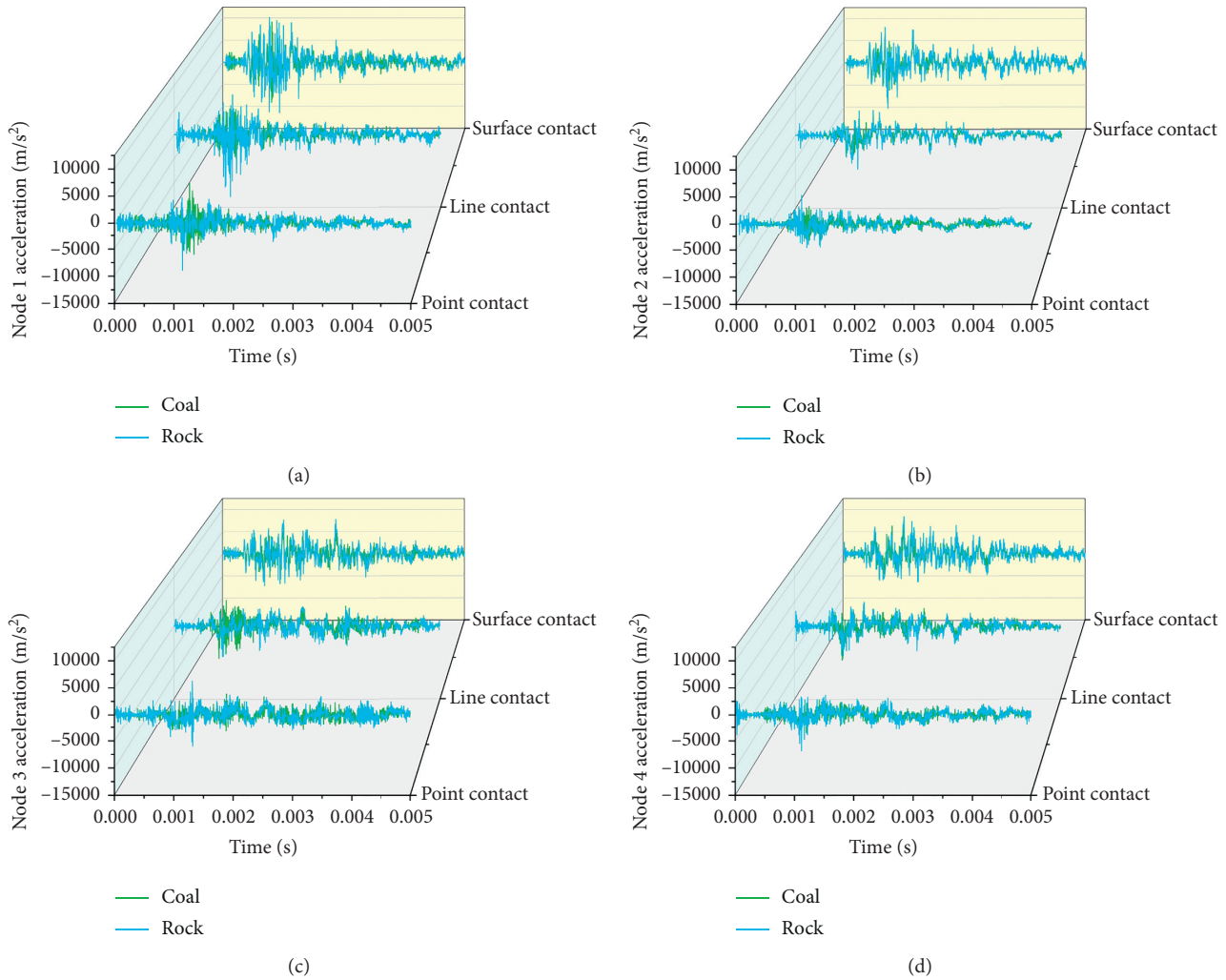

Figure 19: Nodal acceleration in the tail beam noncollision contact zone under different contact modes: (a) Node 1 acceleration; (b) Node 2 acceleration; (c) Node 3 acceleration; (d) Node 4 acceleration.

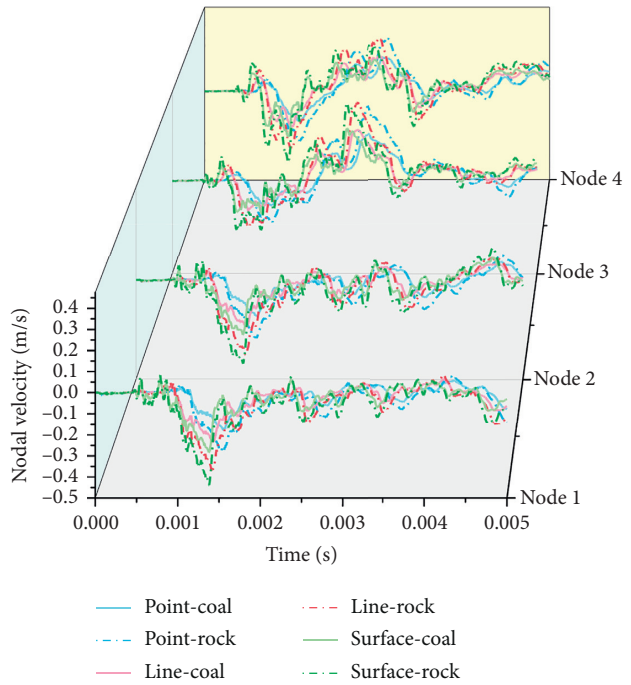

Figure 20: Nodal velocity in the tail beam noncollision contact zone under different contact modes.

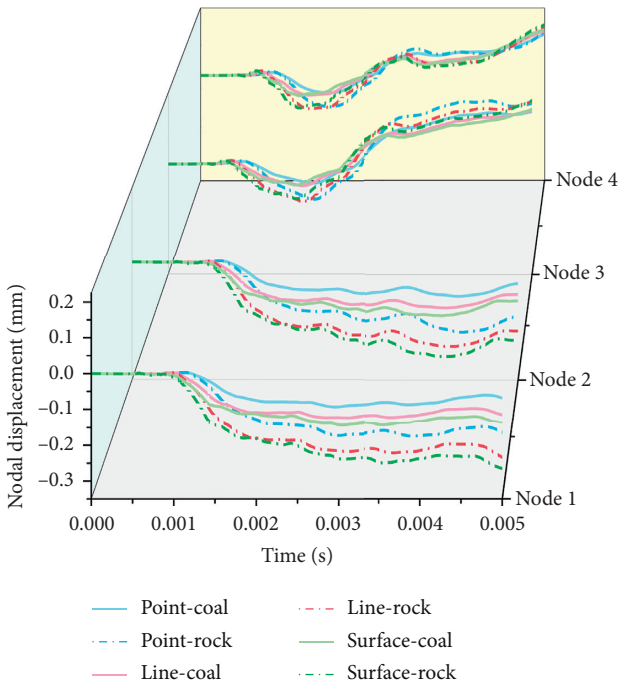

Figure 21: Nodal displacement in the tail beam noncollision contact zone under different contact modes.

and peak value of nodal velocity are in the middle. When the coal-rock particles impact the box structure-based tail beam with the same contact mode, the peak value of the nodal velocity curve in the tail beam noncollision contact zone under the impact of the rock particle is significantly higher than that under the impact of the coal particle. And, the peak value difference is the largest in the surface contact, the second in the line contact, and the smallest in the point contact.

It can be seen from Figure 21 that when the coal-rock particles impact the box structure-based tail beam with different contact modes, the nodal displacement are all shown as follows: the displacement of the upper node of the box structure-based tail beam is the smallest during the point contact, displacement is the largest during the surface contact, and displacement is centered during the line contact, but the influence of the contact mode on the displacement of the lower node of the box structure-based tail beam is not obvious. When the contact mode is the same, the nodal displacement in the tail beam noncollision contact zone under the impact of the rock particle is always greater than that under the impact of the coal particle.

5. Conclusions

In this paper, through the establishment of a simulation model of the coal-rock single particle elastic impacting the box structure-based tail beam, the difference of impact response between the coal particle and rock particle impacting the box structure-based tail beam is studied, and the influence of impact speed and contact mode on the difference was further studied. The conclusion is as follows:

(1) There are differences in the impact response of the box structure-based tail beam under the impact of the coal-rock particle. Under the impact of the rock particle, the velocity peak value of the tail beam contact collision zone is larger, internal energy and kinetic energy of the system are higher, and peak values of acceleration and velocity in the nonimpact contact zone are larger. The impact response of the box structure-based tail beam under the impact of the rock particle is obviously stronger than that under the impact of the coal particle.

(2) When the impact speed of the coal-rock particle increases, the system kinetic energy and internal energy under the impact of the coal-rock particle continue to increase, velocity peak value increases, and response is more rapid in the tail beam collision contact zone, and the vibration amplitude of acceleration and velocity and the nodal displacement increase in the tail beam noncollision contact zone, and the difference of vibration response between the rock particle and coal particle impacting the box structure-based tail beam is more significant. And, the change of impact speed will not change the overall trend of vibration response of the box structure-based box tail beam.

(3) When the impact contact mode between the particles and box structure-based tail beam is point contact, the residual kinetic energy of the system is the most, internal energy of the system is the smallest, dynamic response of the tail beam collision contact zone, and tail beam noncollision contact zone is the weakest, and the impact response difference of the box structure-based tail beam under the impact of the coal-rock particle is the smallest. When the impact contact mode is surface contact, the residual kinetic energy of the system is the least, internal energy of the system is the largest, dynamic response of the tail beam collision contact zone and noncollision contact zone is the strongest, and impact response difference of the box structure-based tail beam under the impact of the coal-rock particle is the largest. When the impact contact mode is line contact, the residual kinetic energy and internal energy of the system are between the former two, and the dynamic response degree of the tail beam collision contact zone and noncollision contact zone is between the former two.

In this paper, the impact of the single coal-rock particle on the box structure-based tail beam is studied, which

provides a reference for further study on the vibration response of the box structure-based tail beam impacted by multiple coal-rock particles. The response difference between the coal-rock particles impacting the box structure-based tail beam provides a basis for coal-rock identification based on the vibration signal in the process of caving coal.

Data Availability

The data used to support the findings of this study are included within the article.

Conflicts of Interest

The authors declare that there are no conflicts of interest regarding the publication of this paper.

Acknowledgments

This work was supported by National Natural Science Foundation of China (Grant no. 51974170) and Special Funds for Climbing Project of Taishan Scholars.

References

[1] Ministry of natural resources of the people's Republic of China, *China Mineral Resources Report*, Geological Publishing House, Beijing, China, 2019.

[2] N. Zhang, C. Liu, and P. Yang, "Flow of top coal and roof rock and loss of top coal in fully mechanized top coal caving mining of extra thick coal seams," *Arabian Journal of Geosciences*, vol. 9, no. 6, p. 465, 2016.

[3] J. Dai, P. Shan, and Q. Zhou, "Study on intelligent identification method of coal pillar stability in fully mechanized caving face of thick coal seam," *Energies*, vol. 13, no. 2, pp. 305–317, 2020.

[4] P. Huang, F. Ju, K. Jessu, M. Xiao, and S. Guo, "Optimization and practice of support working resistance in fully-mechanized top coal caving in shallow thick seam," *Energies*, vol. 10, no. 9, p. 1406, 2017.

[5] D. Zhang, "Discovery on fully mechanized mining equipment nationalization of mine with annual production over 10 million tons," *Coal Science and Technology*, vol. 46, no. 2, pp. 203–207, 2018.

[6] A. Vakili and B. K. Hebblewhite, "A new cavability assessment criterion for longwall top coal caving," *International Journal of Rock Mechanics and Mining Sciences*, vol. 47, no. 8, pp. 1317–1329, 2010.

[7] Y. Xu, S. Li, G. Wang et al., "Intelligent technology of first-mining face of longwall top-coal caving with super large cutting height in extra-thick and hard coal seam," *Coal Science and Technology*, vol. 48, no. 7, pp. 186–194, 2020.

[8] W. Wang and C. Zhang, "Separating coal and gangue using three-dimensional laser scanning," *International Journal of Mineral Processing*, vol. 169, pp. 79–84, 2017.

[9] W. Hou, "Identification of coal and gangue by feed-forward neural network based on data analysis," *International Journal of Coal Preparation and Utilization*, vol. 39, no. 1, pp. 33–43, 2019.

[10] J. Sun and J. She, "Coal-rock image feature extraction and recognition based on support vector machine," *Journal of China Coal Society*, vol. 38, no. S2, pp. 508–512, 2013.

[11] J. Sun and B. Su, "Coal-rock interface detection on the basis of image texture features," *International Journal of Mining Science and Technology*, vol. 23, no. 5, p. 681, 2013.

[12] D. He, B. T. Le, D. Xiao, Y. Mao, F. Shan, and T. T. L. Ha, "Coal mine area monitoring method by machine learning and multispectral remote sensing images," *Infrared Physics & Technology*, vol. 103, p. 103070, 2019.

[13] Y. Mao, B. T. Le, D. Xiao et al., "Coal classification method based on visible-infrared spectroscopy and an improved multilayer extreme learning machine," *Optics & Laser Technology*, vol. 114, pp. 10–15, 2019.

[14] B. T. Le, D. Xiao, Y. Mao, and D. He, "Coal analysis based on visible-infrared spectroscopy and a deep neural network," *Infrared Physics & Technology*, vol. 93, pp. 34–40, 2018.

[15] D. Dou, W. Wu, J. Yang, and Y. Zhang, "Classification of coal and gangue under multiple surface conditions via machine vision and relief-SVM," *Powder Technology*, vol. 356, pp. 1024–1028, 2019.

[16] Z. Zhang, Y. Liu, Q. Hu et al., "Multi-information online detection of coal quality based on machine vision," *Powder Technology*, vol. 374, pp. 250–262, 2020.

[17] Si Lei, Z. Wang, C. Tan, and X. Liu, "A novel approach for coal seam terrain prediction through information fusion of improved D-S evidence theory and neural network," *Measurement*, vol. 54, pp. 140–151, 2014.

[18] Si Lei, Z. Wang, and G. Jiang, "Fusion recognition of shearer coal-rock cutting state based on improved RBF neural network and D-S evidence theory," *IEEE Access*, vol. 7, pp. 122106–122121, 2019.

[19] W. Liu and Y. Yan, "Coal gangue interface detection based on IMF energy and SVM," *International Journal of Digital Content Technology and Its Applications*, vol. 5, no. 4, pp. 160–166, 2011.

[20] W. Liu, K. He, C.-Y. Liu, Q. Gao, and Y.-h. Yan, "Coal-gangue interface detection based on Hilbert spectral analysis of vibrations due to rock impacts on a longwall mining machine," *Proceedings of the Institution of Mechanical Engineers, Part C: Journal of Mechanical Engineering Science*, vol. 229, no. 8, pp. 1523–1531, 2015.

[21] Y. Li, S. Fu, Y. Jiao, and M. Wu, "Collapsing coal-rock identification based on fractal box dimension and wavelet packet energy moment," *Journal of China Coal Society*, vol. 42, no. 03, pp. 803–808, 2017.

[22] H. Wang and Q. Zhang, "Dynamic identification of coal-rock interface based on adaptive weight optimization and multi-sensor information fusion," *Information Fusion*, vol. 51, pp. 114–128, 2019.

[23] Y. Yang, Q. Zeng, L. Wan, and G. Yin, "Dynamic response analysis of the coal gangue-like elastic rock sphere impact on the massless tail beam based on contact-structure theory and FEM," *Shock and Vibration*, vol. 2019, Article ID 6030542, 24 pages, 2019.

[24] Y. Yang, Q. Zeng, G. Yin, and L. Wan, "Vibration test of single coal gangue particle directly impacting the metal plate and the study of coal gangue recognition based on vibration signal and stacking integration," *IEEE Access*, vol. 7, pp. 106784–106805, 2019.

[25] Y. Tian and F. Tian, "Development status and prospect of coal gangue recognition technology in top-coal caving," *Coal Engineering*, vol. 50, no. 10, pp. 142–145, 2018.

[26] H. A. Sherif and F. A. Almufadi, "Identification of contact parameters from elastic-plastic impact of hard sphere and elastic half space," *Wear*, vol. 368-369, pp. 358–367, 2016.

[27] G. K. P. Barrios, R. M. de Carvalho, A. Kwade, L. M. Tavares, and L. M. Tavares, "Contact parameter estimation for DEM simulation of iron ore pellet handling," *Powder Technology*, vol. 248, pp. 84–93, 2013.

[28] P. Flores, M. Machado, M. T. Silva, J. M. Martins, and M. Martins, "On the continuous contact force models for soft materials in multibody dynamics," *Multibody System Dynamics*, vol. 25, no. 3, pp. 357–375, 2011.

[29] L. Skrinjar, J. Slavič, and M. Boltežar, "A review of continuous contact-force models in multibody dynamics," *International Journal of Mechanical Sciences*, vol. 145, pp. 171–187, 2018.

[30] Y. Yang, Q. Zeng, L. Wan, and G. Yin, "Influence of coal gangue volume mixing ratio on the system contact response when multiple coal gangue particles impacting the metal plate and the study of coal gangue mixing ratio recognition based on the metal plate contact response and the multi-information fusion," *IEEE Access*, vol. 8, pp. 102373–102398, 2020.

[31] G.-W. Jang and Y. Y. Kim, "Higher-order in-plane bending analysis of box beams connected at an angled joint considering cross-sectional bending warping and distortion," *Thin-Walled Structures*, vol. 47, no. 12, pp. 1478–1489, 2009.

[32] W. Wang, F. Zhu, S. Sun, T. Liu, and Ge Guo, "Study on seismic behavior of steel box side beam connected to steel box column with linear strengthened through diaphragm," *Journal of Building Structures*, vol. 37, no. 11, pp. 186–194, 2016.